BMC Genomics

RESEARCH Open Access

# Genome-wide identification of *SHMT* family genes in alfalfa (*Medicago sativa*) and its functional analyses under various abiotic stresses

Rong Gao[1], Lijuan Chen[1], Fenqi Chen[1] and Huiling Ma[1*]

## Abstract

**Background** Alfalfa (*Medicago sativa* L.) is the most widely planted legume forage and one of the most economically valuable crops in the world. Serine hydroxymethyltransferase (SHMT), a pyridoxal phosphate-dependent enzyme, plays crucial roles in plant growth, development, and stress responses. To date, there has been no comprehensive bioinformatics investigation conducted on the *SHMT* genes in *M. sativa*.

**Results** Here, we systematically analyzed the phylogenetic relationship, expansion pattern, gene structure, *cis*-acting elements, and expression profile of the *MsSHMT* family genes. The result showed that a total of 15 *SHMT* members were identified from the *M. sativa* genome database. Phylogenetic analysis demonstrated that the *MsSHMT*s can be divided into 4 subgroups and conserved with other plant homologues. Gene structure analysis found that the exons of *MsSHMTs* ranges from 3 to 15. Analysis of *cis*-acting elements found that each of the *MsSHMT* genes contained different kinds of hormones and stress-related *cis*-acting elements in their promoter regions. Expression and function analysis revealed that *MsSHMTs* expressed in all plant tissues. qRT-PCR analysis showed that *MsSHMTs* induced by ABA, Salt, and drought stresses.

**Conclusions** These results provided definite evidence that *MsSHMTs* might involve in growth, development and adversity responses in *M. sativa*, which laid a foundation for future functional studies of *MsSHMTs*.

**Keywords** *Medicago sativa*, Serine hydroxymethyltransferase, Hormones, Abiotic stresses

*Correspondence:
Huiling Ma
mahl@gsau.edu.cn
[1]College of Pratacultural Science, Key Laboratory of Grassland Ecosystem, Ministry of Education, Pratacultural Engineering Laboratory of Gansu Province, Sino-U.S. Center for Grazingland Ecosystem Sustainability, Gansu Agricultural University (36.0° N, 103 8° E), Yingmencun, Anning District, Gansu province, Lanzhou, Gansu 730070, China

## Introduction

Alfalfa (*Medicago sativa* L.), originally from southwestern Asia, is a perennial legume widely grown around the world as an economic forage, and is known as the "King of Forages". Alfalfa is rich in protein, vitamins, flavonoids and other nutrients [1]. In addition, alfalfa has a well-developed root system, and its rhizobacteria can not only provide nitrogen nutrition for plants, but also increase soil fertility and improve soil structure, so it has become the preferred pasture for ecological projects such as returning farmland to grassland, management of wind and sand sources, and soil and water conservation. In recent years, with the change of global climate and soil, the development of alfalfa industry is seriously limited by adverse environmental conditions [2]. During the seedling stage, salinity stress resulted in a significant decrease in root length, root surface area, and root volume of alfalfa [3]. In addition, high salt concentrations resulted in water loss from leaf cells, reduced primary cell elongation, decreased growth rate, and significantly reduced leaf area [4]. Maroua et al. found that under abiotic stress, alfalfa not only has a significant decrease in fresh weight and dry weight yield, but also a significant decrease in protein content [5].

Serine hydroxymethyltransferase (SHMT, EC 2.1.2.1), a pyridoxal phosphate-dependent enzyme, catalyzes the interconversion and reversible hydroxymethyl transfer between L-serine/glycine and tetrahydrofolate ($H_4$PteGlun, THF)/5,10-methylenetetrahydrofolate (5,10-$CH_2$-$H_4$PteGlun). To date, *SHMTs* have been reported in various plants, including *A. thaliana* [6], *S. lycopersicum* [7], *G. max* [8], *O. sativa* [9], *T. aestivum* [10], *M. truncatula* [11], *C. sativus* [12], and P. *trichocarpa* [13]. Research has revealed that *SHMTs* are distributed across multiple cellular compartments, including mitochondria, cytoplasm, chloroplast, and the nucleus [14]. Mitochondrial-localized *SHMT* has been extensively studied, particularly in *A. thaliana*, where *SHMT1* regulates sucrose accumulation and reactive oxygen species (ROS) homeostasis, crucial for primary root growth [15]. Reducing the protein activity of SHMT1 by controlling the level of phosphorylation at S31 leads to decreased metabolic levels, proline and polyamine accumulation, and stomatal closure, which reduces salt tolerance in *A. thaliana* [6]. Heterologous overexpression of *AtSHMT1* promotes formaldehyde metabolism in tobacco leaves. Additionally, co-overexpression of *AtSHMT1* and *AtFDH* induces sugar synthesis and enhances the role of original pathways during formaldehyde metabolism in tobacco [16]. In most cases, mitochondrial SHMT engages in the formation of multiprotein complexes, thereby participating in plant growth, development, and stress response processes. For instance, the mitochondrial SlSHMT interacts with chaperonin 60α1 (SlCPN60α1) to regulate the process of photosynthesis and photorespiration in *S. lycopersicum*es [17]. GmSHMT08 forms a multiprotein complex with soluble NSF attachment protein GmSNAP18 and pathogenesis-related protein GmPR08-Bet VI, maintaining cellular redox homeostasis and conferring resistance to *G. max* cyst nematode (SCN) [18]. OsSHMT1 forms a multiprotein complex with NLR protein OsRSR1, providing resistance against *O. sativa* sheath blight disease [19]. Research on the functionality of *SHMT* in other cellular has been relatively limited. The *OsSHMT* located in the endoplasmic reticulum (ER) enhances cold tolerance in *O. sativa* by interacting with APX and heat shock protein 70 (Hsp70), facilitating the removal of excess $H_2O_2$ in plants [20]. Moreover, transient silencing of *TaSHMT3A-1* reduces T. aestivum resistance to fusarium head blight [10]. A study on *PtSHMT2* localized in the cytoplasm showed its high expression levels within the wood tissue during *P. trichocarpa* development and demonstrated that overexpression *PtSHMT2* enhances *P. trichocarpa* growth through increased biomass production and the release of sugars (glucose and xylose) [13].

No *SHMT* family member in *M. sativa* has been characterized till date. Thus, in order to discover the genetic evolution and function of *SHMT* gene family in *M. sativa*, we utilized the published genomic information of *M. sativa* (cultivar XinJiangDaYe) to identify members of the *MsSHMT* genes. The expansion patterns, evolutionary relationships, gene structures, conserved motifs, *cis*-acting elements, as well as tissue-specific expression patterns of the *MsSHMTs* were systematically analyzed. Additionally, the response patterns of the *MsSHMT* genes to harmonizes and stresses were analyzed using qRT-PCR. These findings establish a theoretical foundation for understanding the functionality of *MsSHMTs* and provide important candidate genes for resistance studies in *M. sativa*.

## Materials and methods

### Identification of the *SHMT* gene family in *M. sativa*

First, we obtained the Hidden Markov Model (HMM) of the SHMT domain (PF00464) from the Pfam database (https://pfam.xfam.org/, accessed on 22 August 2023). Meanwhile, the genome assembly files of *M. sativa* (cultivar XinJiangDaYe, Released in December 2020) were downloaded from the figshare projects (https://figshare.com/projects/whole_genome_sequencing_and_assembly_of_Medicago_sativa/66380, accessed on 22 August 2023) [21]. Then, taking the HMM of SHMT as a template, we utilized HMMER to query the candidate proteins from the *M. sativa* database with an e-value cut-off of $e^{-10}$. The redundant sequences of candidate proteins were removed using the CD-Hit with threshold 90% [22]. The physical and chemical properties were analyzed by

Expasy (https://web.expasy.org/protparam/, accessed on 28 August 2023) [23]. Subcellular localization was predicted using the online website WOLF-PSORT (https://wolfpsort.hgc.jp/, accessed on 28 August 2023).

#### Exon-Intron structure analysis and conserved motifs identification

The exon-intron structure information of *MsSHMTs* was extracted from the *M. sativa* general feature format (GFF) file. The conserved motif of MsSHMTs was identified by the online tool MEME (https://meme-suite.org/meme/, accessed on 10 September 2023), with default setting except for changes in the number of motifs to 10 [24]. Results were visualized using TBtools.

#### Phylogenetic analysis

A total of 76 SHMT protein sequences from *A. thaliana* (7), *G. max* (13), *O. sativa* (5), *P. trichocarpa* (9), *S. lycopersicum* (7), *C. sativus* (6), *T. aestivum* (14), and *M. sativa* (15) were downloaded from TAIR (Arabidopsis thaliana. org/, accessed on 15 September 2023) and Phytozome database (https://phytozome-next.jgi.doe.gov/, accessed on 15 September 2023). The multiple sequence alignment was performed using the ClustalW with the default settings. The phylogenetic tree based on neighbor-joining (NJ) method was constructed using MEGA-X software with bootstrap values from 1,000 replicates indicated at each node. The constructed phylogenetic tree was embellished using website ChiPlot (https://www.chiplot.online/, accessed on 20 September 2023).

#### Gene synteny analysis and *MsSHMTs* paralogs gene pair identification

One step MCScanX was employed to identify putative homologous chromosomal regions within and between *M. sativa* with the default parameters. Collinearity results within *M. sativa* genome were mapped using advanced circus software in TBtools. Multiple synteny plot was used to show the synteny relationship of the orthologous *SHMT* genes obtained from *M. sativa*, *A. thaliana*, and *G. max* [25].

#### *Cis*-elements in the upstream of *MsSHMTs*

The upstream 2000 bp sequences of the *MsSHMTs* coding region were retrieved from the *M. sativa* genomic database and submitted to PlantCARE (http://bioinformatics.psb.ugent.be/webtools/plantcare/html, accessed on 21 September 2023) to identify regulatory elements involved in hormone and stress responses. The result was visualized with ChiPlot (accessed on 21 September 2023).

#### Analysis of *MsSHMTs* expression pattern in different tissues

The RNA-seq data on different tissues of *M. sativa* were downloaded from the NCBI short read archive database as accession SRP055547 [26]. The genes corresponding to the XinJiangDaYe *MsSHMTs* were screened by online Blast (https://medicago.legumeinfo.org/, accessed on 2 October 2023). Expression data of six tissues including flowers, leaves, pre-elongating stems, elongating stems, roots, and nodules were normalized and visualized using the pheatmap R package. Genes with significantly higher expression levels in a specific tissue compared to others are considered tissue-specific genes ($p<0.05$).

#### Plant materials, growth conditions, and treatments

Alfalfa (cultivar Gannong NO.3) was provided by the Gansu Agricultural University, Lanzhou, China. We selected full and consistent seeds, sterilized them with 6% NaClO for 5 min, evenly distributed the seeds onto vermiculite, and placed them in a photoperiodic growth chamber for cultivation. The temperature during cultivation should be maintained at 25/20℃ (day/night), with a 14/10 h (light/dark) cycle. 6 days after sowing, the *M. sativa* seedlings were transplanted into 1/2 Hoagland nutrient solution for hydroponics. When the seeds were 4 weeks of age, seedlings with uniform growth were treated with ABA (100 μM), SA (100 μM), MeJA (100 μM), drought (20% PEG6000), salt (200 mM NaCl), alkali (150 mM $NaHCO_3$), and low (4 °C) and high (37 °C) temperatures. Samples were collected at 0 h (CK) and 3 h, 6 h, 12 h, 24 h, and 48 h after treatment. All sample collections were set up with three biological replicates. The samples were quickly frozen in liquid nitrogen after sampling, then transferred to -80 °C, and stored for subsequent analysis.

#### RNA extraction and real-time quantitative PCR

Total RNA was extracted from the samples using TRIzol reagent (Invitrogen, Carlsbad, CA, USA). The FastQuant First Strand cDNA Synthesis Kit (Tiangen, Beijing, China).

was used to synthesize cDNA. qRT PCR was carried out using the LightCycler 480 Real-Time PCR System (Roche Applied Science) and SYBR® Green Premix Pro Taq HS qPCR Kit. Three biological replicates with three technical replicates each were performed. The primers were designed by Primer 5.0 software and listed in Table 1. The reference gene is *MsActin* (MS.gene049321.t1). The $2^{-\Delta\Delta CT}$ calculation method was used to quantify the relative expression of the target gene.

## Result

#### Identification and characterization of *MsSHMTs* in *M. sativa*

As shown in Table 2, a total of 15 *MsSHMT* genes were identified in the *M. sativa* genomes. Basic information analysis found that *MsSHMTs* are unevenly located on chromosomes. The protein length of the MsSHMTs ranges from 593 (MsSHMT5) to 99 (MsSHMT14)

**Table 1** Primers used for qRT-PCR analysis

| Gene name | Forward primer(5′-3′) | Reverse primer(5′-3′) |
|---|---|---|
| *MsSHMT1* | CTGAGCGCCAAACTTCTGG | TGCCATTGTCACCTCCGG |
| *MsSHMT2* | TCATGGACCACGTGGAGC | TCCCACCAGAAACAAG CTCG |
| *MsSHMT3* | GGTATTGATGGTGCTTTGGTG | AACCAAGCCAAATACTC CGTG |
| *MsSHMT4* | ATTGCTGGTGCCAGTGCT | GCCCACTTACGTGAGCCA |
| *MsSHMT5* | CAAAACCAAGGAAGAGAGG | ACAGAGCAGATGCTAA AGC |
| *MsSHMT6* | GAGGACTAAAGGATTCACG | GATTTTCACTACCACCAGA |
| *MsSHMT7* | GGGGTAACTACACAATTGG AGG | ACTCCGGGAATAGGAT ACTG |
| *MsSHMT8* | ATTACCAAAAGCAGGTGG TTCC | TCACTCACCAGGCACAA AATTC |
| *MsSHMT9* | GGTTCTATTTCTTCGGGAGG | TGGGAGCCAAATGTCT CAAC |
| *MsSHMT10* | CTCTTGGCTTGACCGGCA | GGGCCAAGGCACTGCTAT |
| *MsSHMT11* | ATGCACGCATTCGCAAGG | ACCAGCTGCAACCAGTCC |
| *MsSHMT12* | ACTTTGACGCGGCTGTCA | CATGGCGGAGATCAGCGA |
| *MsSHMT13* | CGCGGCTGTCAGAATTGC | TTCACGGCGGAGATCAGC |
| *MsSHMT14* | CTCCGGTAGCGGGTTGTC | AGCAACCACCTGCACACT |
| *MsSHMT15* | AAGGTTCCGTGCATGGGG | GTGTGGAGATGCGGACCC |
| *MsActin* | GACAATGGAACTGGAATGG | CAATACCGTGCTCAATGG |

amino acids (aa), with corresponding molecular weights of 11.33 kDa and 65.98 kDa, respectively. Physicochemical property analysis showed that the isoelectric points of MsSHMTs are concentrated between 5.29 (MsSHMT15) and 9.35 (MsSHMT2), with most of them being neutral and basic proteins. The instability index analysis found that most of MsSHMT proteins are stable (Instability index < 40) except MsSHMT1, 5, and 11. In addition, 93% of MsSHMT proteins are hydrophilic (GRAVY < 0). Subcellular localization prediction revealed that MsSHMTs are distributed in the mitochondrial, Cytoplasmic, vacuole, and Chloroplast, where MsSHMT1/2/8/14/15 are cytoplasmic localization proteins, MsSHMT4/5/6/9/10 are chloroplast localization proteins, and MsSHMT11/12 are mitochondrial localization proteins.

### Phylogenetic analysis of *SHMT* gene family

To study the evolutionary history of the *SHMT* gene family in *M. sativa*, we constructed a phylogenetic tree from the alignment of 76 full-length SHMT protein sequences in model monocotyledon and dicotyledonous using the NJ method. The results revealed that SHMTs can be categorized into 4 distinct classes (Class I-IV), encompassing 21, 18, 15, and 22 proteins, respectively (Fig. 1). Notably, MsSHMT proteins are present in all classes. Class I consists of 5 TaSHMTs, 4 GmSHMTs, 3 PtrSHMTs, 2 MsSHMTs/AtSHMT/CsSHMTs/OsSHMTs, and 1 SlSHMT. Within Class II, MsSHMT10 is highly homologous to GmSHMT05c and GmSHMT08c. Class III contains 8 MsSHMHT members (MsSHMT2/3/4/6/7/8/14/15), which displayed the highest level of homology with GmSHMTs, AtSHMTs, and SlSHMTs, while OsSHMT proteins are absent. In Class IV, 4 members of the MsSHMT family, MsSHMT1/11/12/13, exhibit relatively close evolutionary relationships with GmSHMT02m, GmSHMT14m, GmSHMT08m, and GmSHMT18m.

### Synteny analysis of *MsSHMT* genes in *M. sativa*, *Arabidpsis*, and *G. max*

To explore the expansion patterns of *M. sativa* SHMT genes, we embarked on the relationship between *M. sativa SHMT* gene sequences. The analysis unveiled

**Table 2** Basic information of 15 *MsSHMTs* identified in this study

| Gene name | Gene ID | Chr | Gene location | Protein length(aa) | MW (Da) | pI | Instability index: | GRAVY | Predicted localization |
|---|---|---|---|---|---|---|---|---|---|
| *MsSHMT1* | MS.gene054086.t1 | Chr1.3 | 13,898,473–13,900,628 | 269 | 29385.69 | 7.13 | 42.71 | -0.185 | Cytoplasmic |
| *MsSHMT2* | MS.gene21342.t1 | Chr1.4 | 71,261,850–71,265,740 | 312 | 34724.83 | 9.35 | 29.89 | 0.065 | Cytoplasmic |
| *MsSHMT3* | MS.gene00142.t1 | Chr2.1 | 58,778,423–58,783,243 | 427 | 47928.53 | 5.53 | 32.45 | -0.152 | Cytoskeleton |
| *MsSHMT4* | MS.gene002678.t1 | Chr2.1 | 68,367,665–68,371,513 | 534 | 57624.67 | 7.07 | 34.78 | -0.128 | Chloroplast |
| *MsSHMT5* | MS.gene00638.t1 | Chr2.1 | 75,602,767–75,605,738 | 593 | 65982.99 | 6.74 | 45.78 | -0.385 | Chloroplast |
| *MsSHMT6* | MS.gene67721.t1 | Chr2.2 | 54,999,137–55,003,137 | 448 | 49971.92 | 6.24 | 32.53 | -0.133 | Chloroplast |
| *MsSHMT7* | MS.gene55974.t1 | Chr2.3 | 56,879,219–56,883,189 | 489 | 55015.23 | 6.09 | 39.78 | -0.02 | Vacuole |
| *MsSHMT8* | MS.gene058253.t1 | Chr2.4 | 56,852,615–56,853,675 | 104 | 11620.36 | 7.87 | 35.26 | -0.172 | Cytoplasmic |
| *MsSHMT9* | MS.gene30747.t1 | Chr3.1 | 60,183,533–60,188,266 | 575 | 63879.34 | 6.23 | 37.24 | -0.363 | Chloroplast |
| *MsSHMT10* | MS.gene79894.t1 | Chr3.1 | 65,415,608–65,417,370 | 471 | 51700.87 | 6.84 | 36.53 | -0.258 | Chloroplast |
| *MsSHMT11* | MS.gene068634.t1 | Chr5.1 | 21,238,333–21,242,799 | 538 | 59523.9 | 8.36 | 41.61 | -0.277 | Mitochondrion |
| *MsSHMT12* | MS.gene21274.t1 | Chr5.1 | 51,970,127–51,978,403 | 507 | 56208.15 | 7.73 | 36.71 | -0.331 | Mitochondrion |
| *MsSHMT13* | MS.gene061524.t1 | Chr5.4 | 52,384,830–52,390,828 | 322 | 35879.05 | 8.24 | 39.84 | -0.265 | Cytoskeleton |
| *MsSHMT14* | MS.gene039450.t1 | Chr6.1 | 37,507,554–37,508,225 | 99 | 11330.22 | 9.34 | 38.64 | -0.167 | Cytoplasmic |
| *MsSHMT15* | MS.gene22990.t1 | Chr7.2 | 6,472,660–6,479,839 | 535 | 59519.29 | 5.29 | 36.21 | -0.234 | Cytoplasmic |

**MW* Molecular weight; *pI* Isoelectric point; *GRAVY* Grand average of hydropathicity

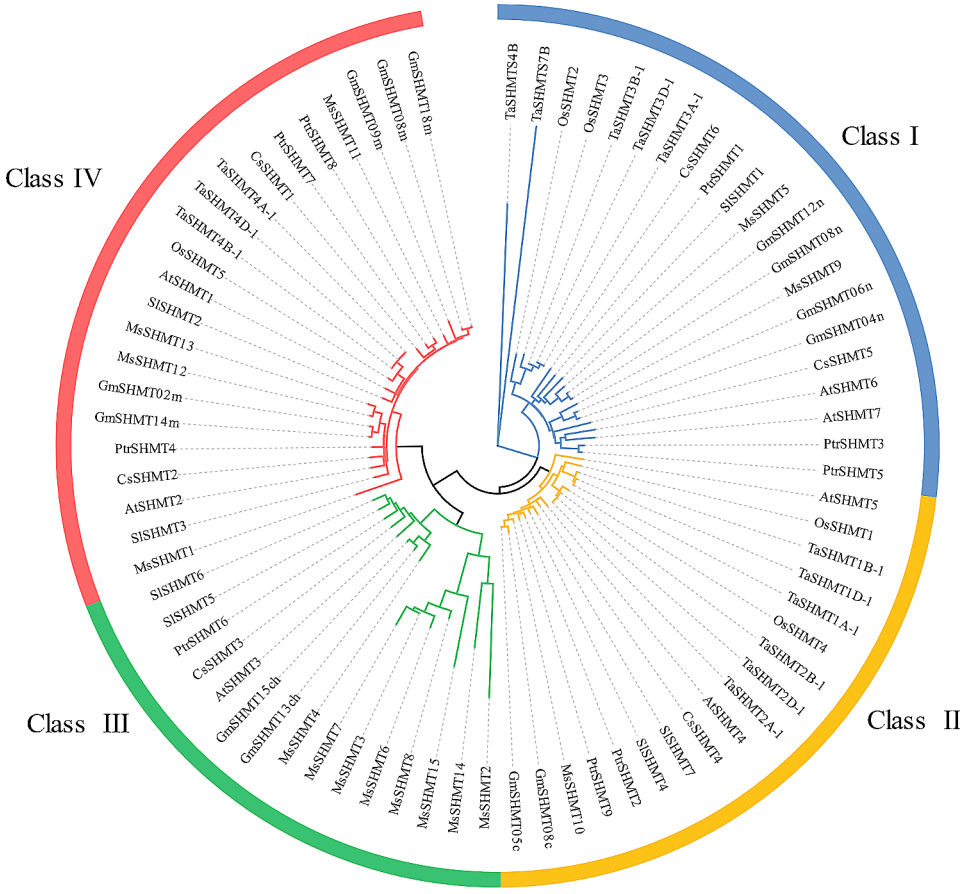


**Fig. 1** Phylogenetic analysis of *SHMT* gene family. The amino acid sequences of SHMT proteins from *O. sativa* (5), *T. aestivum* (14), *A. thaliana* (7), *G. max* (13), *C. sativus* (6), *S. lycopersicum* (7), *P. trichocarpa* (9), and *M. sativa* (15) were used for analysis

the occurrence of 3 fragment duplication event, *MsSHMT3/6*, *MsSHMT3/7*, and *MsSHMT6/7*. However, no occurrences of segmental duplication events were identified (Fig. 2A). The *Ka/Ks* values of these fragment duplication genes are lower than 1, suggesting that *SHMT* family genes evolved mainly under the influence of purifying selection (Supplementary Table S1). Through comparative analysis of the *SHMT* genes genetic relationship between *M. sativa*, *A. thaliana*, and *G. max*, we found 4 orthologous genomic fragments shared between *M. sativa* and *A. thaliana*, along with 11 orthologous fragments shared between *M. sativa* and *G. max* (Fig. 2B). Notably, chromosomes 2.1, 3.1, and 5.1 of *M. sativa* exhibit a higher frequency of homologous segments containing 3, 7, and 5 homologous genes, respectively.

### Gene structure and conserved domain analysis of *MsSHMT* family genes

Based on the gene annotation files, we analyzed the exon-intron structural characteristics of *MsSHMT* genes. As illustrated in Fig. 3A, the number of exons vary in the range of 3 to 15. Among them, *MsSHMT11/12* manifest 15 exons, *MsSHMT2/3/6/13* manifest 10 exons, *MsSHMT5/8/9/10* exhibit 4 exons. *MsSHMT* genes demonstrating highly similar exon-intron structures were clustered within the same clade, for instance, *MsSHMT5/9/10* and *MsSHMT3/6/7*. The investigation of conserved motifs revealed the presence of 10 conserved motifs in the MsSHMTs, with lengths spanning from 11 to 50 amino acids (Supplementary Figure S1). Conserved motifs among the MsSHMTs within a particular clade present a marked resemblance. Nevertheless, certain genes exhibit significant variations in motif composition within the same clade, such as MsSHMT8 and MsSHMT14 (Fig. 3B).

### *Cis*-acting elements in the *MsSHMTs* promoters

To explore the potential functions of *MsSHMTs*, we analyzed the gene's promoter region sequence. The results revealed a significant presence of cis-acting elements in *MsSHMTs*, which can be categorized into two groups: hormone-related and stress-related elements (Fig. 4A). Hormone-associated elements include the ABA-responsive element (ABRE), MeJA-responsive element (CGTCA/TGACG-motif), SA-responsive element (TCA-element), IAA-responsive element (TGA),

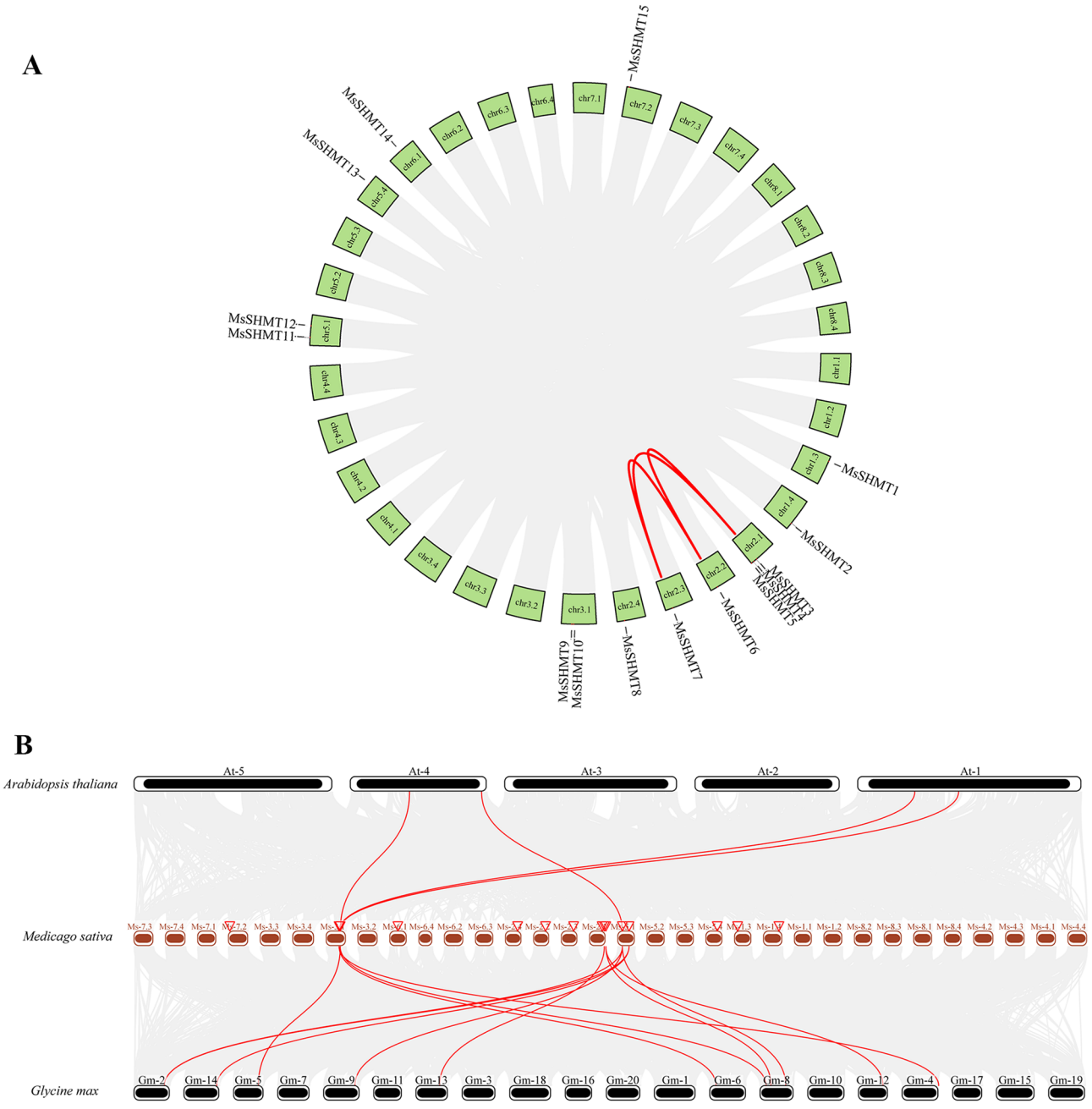


**Fig. 2** Gene duplication and collinearity analysis of *MsSHMTs*. **A**: Schematic representation for the chromosomal distribution and interchromosomal relationships of *MsSHMTs*. Gray lines indicate all synteny blocks in the *M. sativa* genome, and the red line indicates segmental duplication *MsSHMT* gene pairs; **B**: collinear relationships of genes pairs from *M. sativa*, *A. thaliana*, and *G. max*. Gray lines in the background indicate the collinear blocks within *M. sativa*, *A. thaliana*, and *G. max* genomes and red lines indicate the collinear *SHMT* gene pairs

and GA-responsive element (P-box). Stress-associated elements include TC-rich repeat sequences, a drought response element (MBS), a low-temperature response element (LTR), an anaerobic response element (ARE), and a wound-responsive element (WUN-motif). Certain elements are shared among multiple *MsSHMTs* (Fig. 4B). For instance, all *MsSHMTs* except *MsSHMT2/6/9/13* contain ABRE elements. CGTCA-motif and TGACG-motif are present in all *MsSHMTs* except *MsSHMT6*. ARE motifs are found in all *MsSHMTs* except *MsSHMT6*.

### Tissue expression profile analysis of *MsSHMT* genes

To research the role of *MsSHMTs* in the growth and development of *M. sativa*, we analyzed the expression

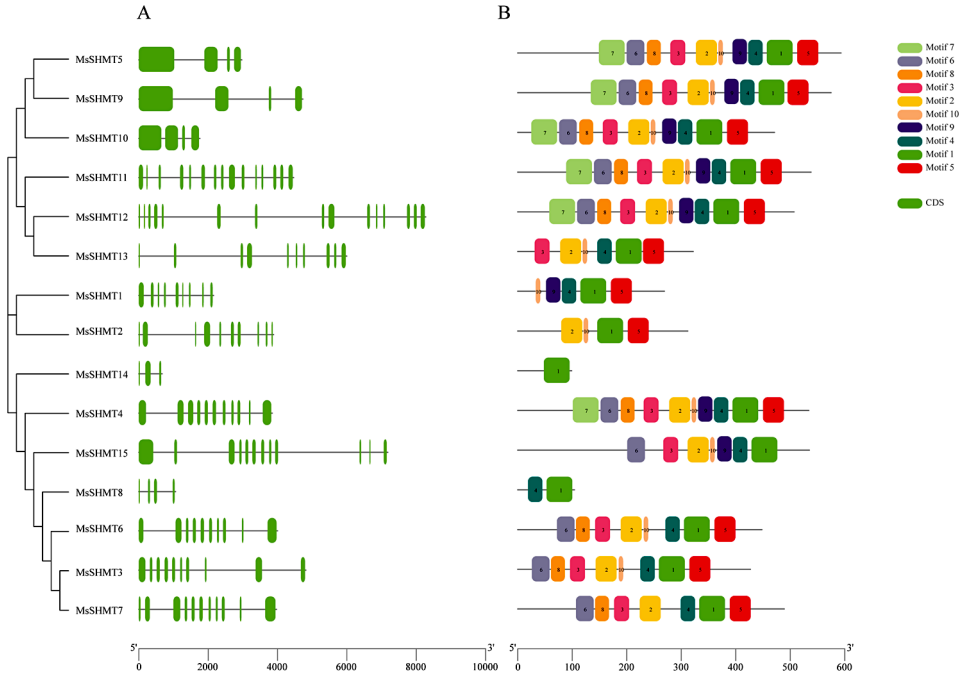


**Fig. 3** Gene structure and conserved domain analysis of *MsSHMTs* in *M. sativa*. **A**: Exon-intron structure of *MsSHMTs*. **B**: Motif distribution of MsSHMT proteins. Different motifs (1–10) are indicated by different colors. The sequence logos and information for each motif are provided in Additional files Figure S1

patterns of the *MsSHMT* genes in various tissues using published transcriptome data. The results indicated that the *MsSHMTs* are expresses in all tissues of *M. sativa* (Fig. 5). However, the expression patterns vary among *MsSHMTs*. In nodules, the expression levels of *MsSHMT4/6/7/14* were the highest. *MsSHMT1/3/9/11* showed high expression in leaves, followed by stems. The expression level of *MsSHMT2* in roots was significantly higher compared to other tissues. *MsSHMT5* exhibited high expression in both roots and flowers. *MsSHMT8/10/12/13/15* displayed high expression levels in both roots and stems. These findings suggest that *MsSHMTs* may play a significant role in the developmental processes of *M. sativa* leaves, roots, and nodules.

### Expression profile analysis of *MsSHMT* genes under hormones

To explore the response patterns of *MsSHMT* members to phytohormones, qRT-PCR was employed to detect the expression profiles of 15 *MsSHMTs* under ABA, SA, and MeJA treatments. The results indicate that transcript levels of all *MsSHMTs* exhibited an initial increase followed by a decrease under ABA treatment (Fig. 6A). Among them, *MsSHMT1/2/10/11/12/13* reached their highest expression level at 3 h, while *MsSHMT3/6/7/8/9/15* peaked at 6 h. Additionally, *MsSHMT5/4/14* demonstrated higher expression levels at 6–12 h. Under SA treatment, the expression levels of *MsSHMT1/2/6/9/11/12/14* were repressed (Fig. 6B). However, other *MsSHMT* members including *MsSHMT4/8/13/10* were up-regulated, reaching their peak expression level at 24 h, and *MsSHMT3/5/7/15* reached their highest expression level at 48 h. Under MeJA treatment, the expression levels of most *MsSHMT* members were inhibited, such as *MsSHMT1/2/3/6/10/14*. However, other members such as *MsSHMT5/15* were up-regulated at 3 h, and *MsSHMT4/7/13* were up-regulated at 24 and 48 h (Fig. 6C).

### Expression profile analysis of *MsSHMT* genes under abiotic stresses

Upon further analysis, it was found that the expression levels of *MsSHMT* genes vary under various abiotic treatments. Regarding *MsSHMT1*, its expression level is down-regulated under alkali and cold treatment, while it is significantly up-regulated under salt, heat, and drought treatments (Fig. 7). In the case of *MsSHMT2*, there is almost no change in expression level under drought and cold treatment, but it is significantly up-regulated under salt, alkali, and heat treatments. *MsSHMT3/5/13* are up-regulated under salt and drought treatments, but remain almost unchanged under cold treatment. Meanwhile, *MsSHMT8* is up-regulated by drought treatment, while its expression is down-regulated under other treatments. *MsSHMT4* is up-regulated under cold and heat treatments, reaching its highest expression level at 12 h. *MsSHMT6/7/9* are up-regulated under drought treatment, reaching their highest expression levels at 24 h, 12 h, and 3 h, respectively. *MsSHMT10* is up-regulated under drought treatment, reaching a higher expression

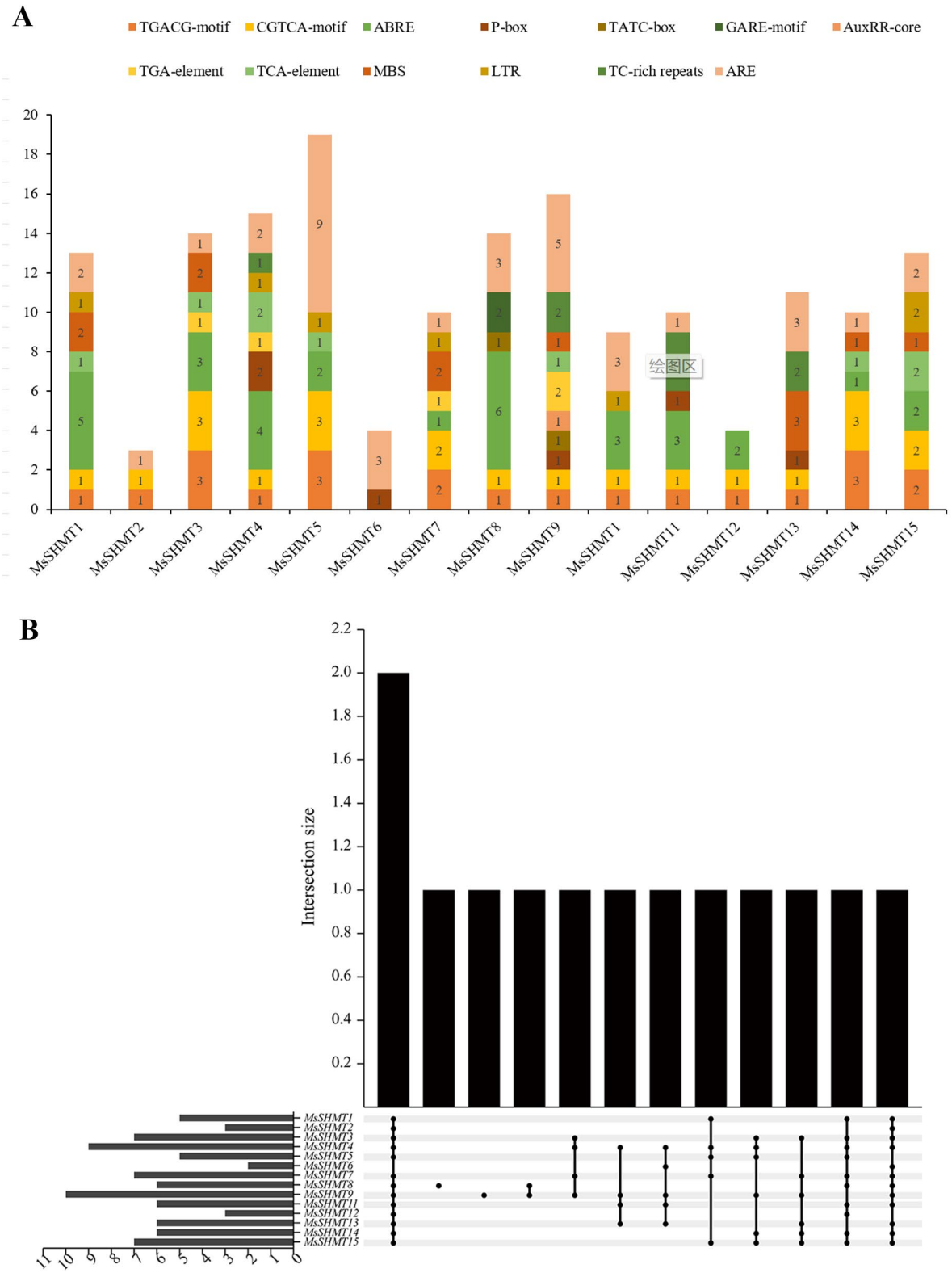


**Fig. 4** Identification of the *cis*-acting element in the 2-kb promoter region of *MsSHMT* genes. (**A**) Statistics on the number of *cis*-acting elements of *MsSHMTs*. (**B**) Analysis of shared *cis*-acting elements of *MsSHMTs*. The numbers on the box represent the count of *cis*-elements in the promoter

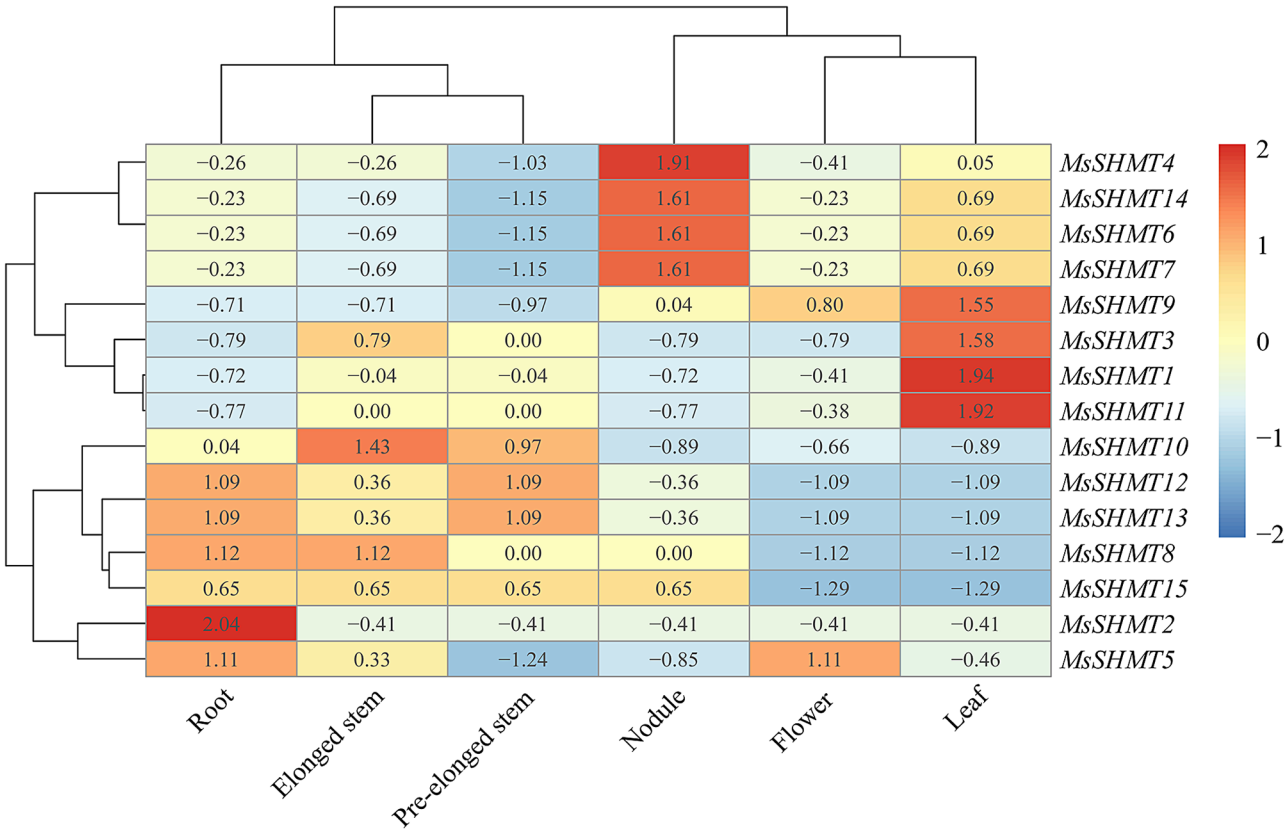


**Fig. 5** Expression patterns of *MsSHMTs* in different tissues of *M. sativa*. The data of transcriptional level comes from the NCBI (accession number: SRP055547). Red and blue represent high and low expression, respectively

level at 3 h, but remains almost unchanged under salt and alkali treatments. *MsSHMT11* is significantly induced by cold stress. *MsSHMT14* is up-regulated under salt and drought treatments, but remains almost unchanged under heat treatment. There is down-regulation of *MsSHMT15* expression level under salt treatment, while it is significantly up-regulated under alkali and drought treatments.

## Discussion

With the release of the *M. sativa* (Zhongmu No. 1 and Xinjiang Daye) genomes, a large number of genes related to stress response and growth development have been explored [21, 27]. Serine hydroxymethyltransferase (SHMT), as an important enzyme shared by both animals and plants, has garnered significant attention from researchers in the field of plant biology. Studies have reported that *G. max* contains 18 members of the *SHMT* gene family, *T. aestivum* has 14, *P. trichocarpa* has 9, *A. thaliana* has 7, *S. lycopersicum* has 7, and *O. sativa* has 5 [7, 10, 13, 20, 28, 29]. In this study, we identified a total of 15 members of the *SHMTs* family in the genome of *M. sativa* (Table 1). This count is close than that of *G. max* and *T. aestivum* but greater than that of *A. thaliana*, *S. lycopersicum*, and *O. sativa*. It appears to be correlated with genome size and the number of whole-genome duplications. Further analysis of the replication event of *MsSHMTs* genes revealed the presence of 3 pair fragment duplication genes (*MsSHMT3/6*, *MsSHMT3/7*, and *MsSHMT6/7*) with a Ka/Ks value of less than 1 (Table S1). This indicates that *MsSHMTs* have undergone purifying selection. Comparison of collinearity relationships between *M. sativa*, *G. max*, and *A. thaliana* revealed that one *MsSHMT* gene corresponds to multiple *GmSHMT* genes, suggesting an independent replication event in *G. max* (Fig. 2) [30]. These results suggest that the expansion of *MsSHMTs* is primarily driven by whole-genome duplication and segmental duplication, consistent with previous research in *G. max*, *T. aestivum*, and *S. lycopersicum* [29].

Evolutionary analysis plays a crucial role in revealing the evolutionary history of gene families, determining orthologous genes, and inferring gene functions, among other aspects [31]. Previous studies have shown that SHMTs can be classified into 4 subclasses based on their location within different organelles: mitochondria, chloroplasts, nucleus, and cytoplasm [32]. This classification is consistent with the findings of this study, where 76 SHMT proteins were classed into 4 subclasses (Fig. 1). However, whether these subclasses are associated with

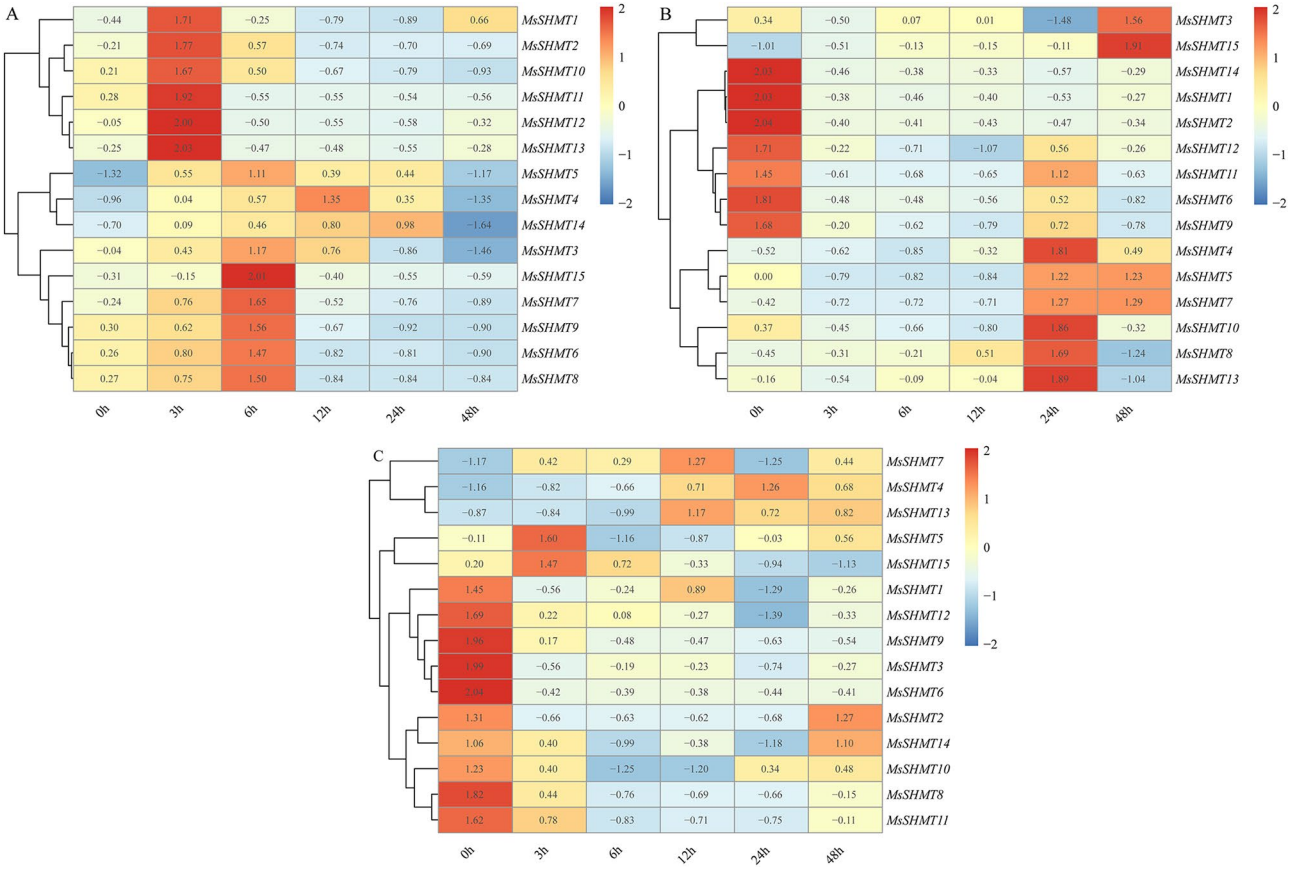


**Fig. 6** Expression levels of *MsSHMT* genes under ABA (**A**), SA (**B**) and MeJA (**C**) treatment. The color scale represents the folding changes normalized by log2 transformed data. Blue represents down-regulated genes and red represents up-regulated genes

distinct subcellular localization of the proteins still requires extensive experimental validation. Furthermore, SHMT activity has been detected in other organelles such as the endoplasmic reticulum [20]. Surprisingly, it has been revealed that a specific *SHMT* gene loss event occurred in some monocotyledonous [29]. In this study, the absence of Class III SHMT in monocotyledonous *O. sativa*, and whole *T. aestivum* did not exhibit this loss in the *SHMT* family. This discrepancy may be attributed to the reduced necessity of Class III *SHMT* genes in *O. sativa* due to long-term genetic evolution. Alternatively, it could be a result of the natural degradation after an accidental gene duplication event, where redundant copies are no longer retained through natural selection [33]. Furthermore, the genes belonging to the same clade exhibit a high similarity in both gene structure and motif composition, as exemplified by *MsSHMT5/9*. However, a subset of genes, such as *MsSHMT8* and *MsSHMT14* displayed significant differences in gene structure. This finding suggests that *SHMTs* are evolutionarily conserved but undergo adaptive structural changes [34]. The number of exons among members of the *M. sativa SHMT* family varies from 3 to 15, indicating *MsSHMT* family maybe experience exon retention or alternative splicing events during evolution [35].

In plants, *SHMT* genes have been identified in numerous tissues [28]. In *A. thaliana*, *AtSHMT1* is predominantly found in leaves, stems, and flowers, while *AtSHMT3* is primarily expressed in germinating seeds, and the transcript accumulation of *AtSHMT4* is restricted to the roots of seedlings [36]. *BvSHMTa* is expressed in both leaves and roots of sugar beets [37]. In *G. maxs*, most *GmSHMT* genes exhibit ubiquitous expression across all tissues [29]. This is consistent with results in *M. sativa* suggesting that the diversification of spatiotemporal expression patterns may represent a common evolutionary feature of the *SHMT* gene family, enabling *SHMTs* to function across various tissues at different growth and developmental stages [38]. Among all the analyzed tissues, the expression of *MsSHMT1/3/9/11* was most highly expressed in leaves, while transcripts of *MsSHMT4/6/7/14* were most expressed in root nodules, and the transcription levels of *MsSHMT2/5/8/13/15* were highly expressed in roots (Fig. 5). These findings indicate that *MsSHMT* genes may play pivotal roles in processes such as leaf photosynthesis, root system stability, and nitrogen fixation in root nodules [39].

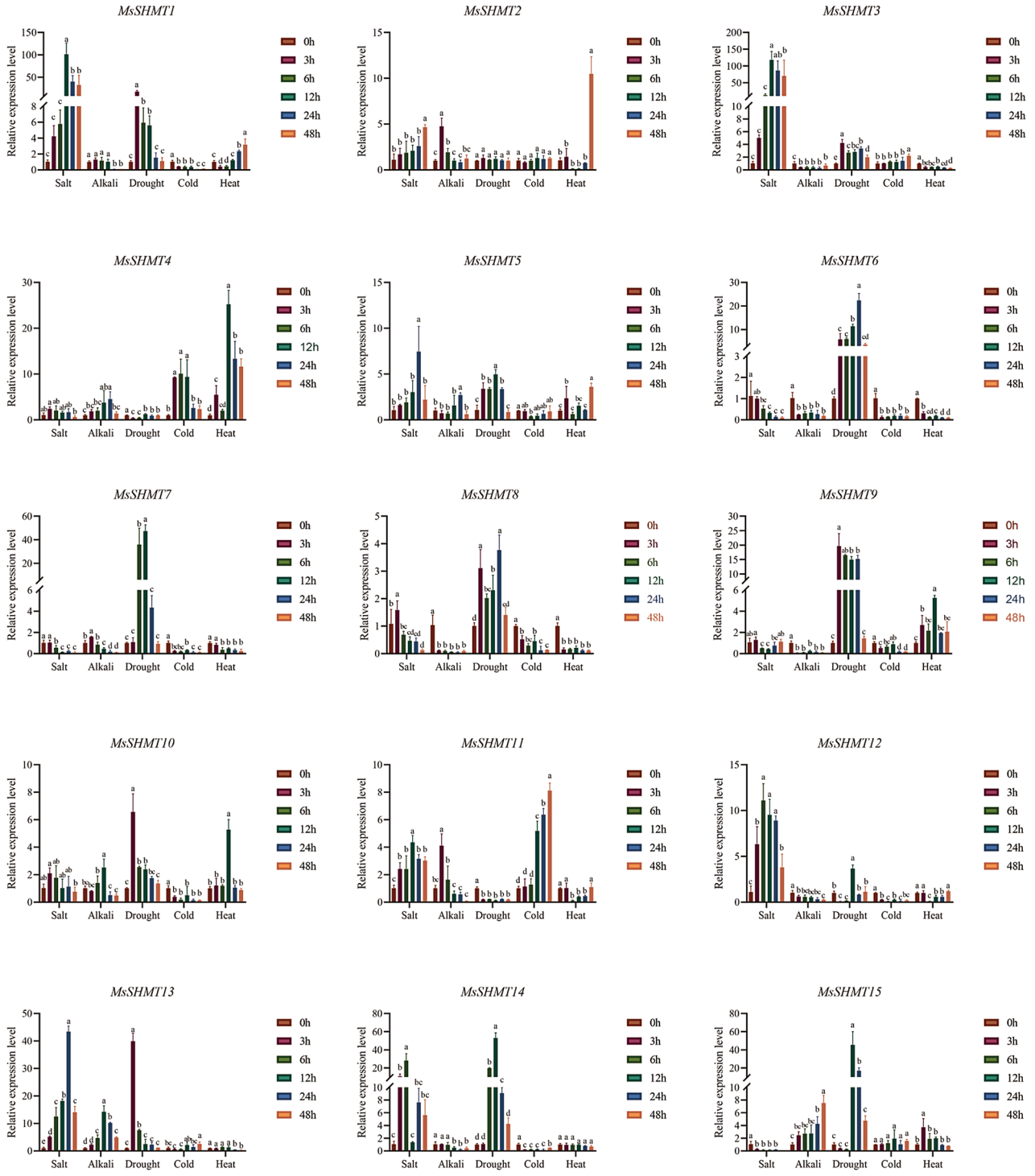


**Fig. 7** qRT-PCR analysis of *MsSHMT* genes in response to salinity, alkali, drought, cold, and heat treatments. All data were expressed as the mean ± standard error (SE) of three independent replicates. Duncan's analytical test ($P < 0.05$) was used to determine the significance of the differences between 0 h

The response of *SHMTs* to hormones has been reported in numerous species [12]. In our study, the *MsSHMT* gene exhibited responses to ABA, SA, and MeJA treatments, suggesting its involvement in hormone regulation and consequently, in controlling the growth and development of *M. sativa* [40]. Additionally, this transcriptional activation may be associated with multiple hormone-responsive elements in the promoter region of the *MsSHMT* genes [41]. However, our further investigations have yielded some conflicting results. For

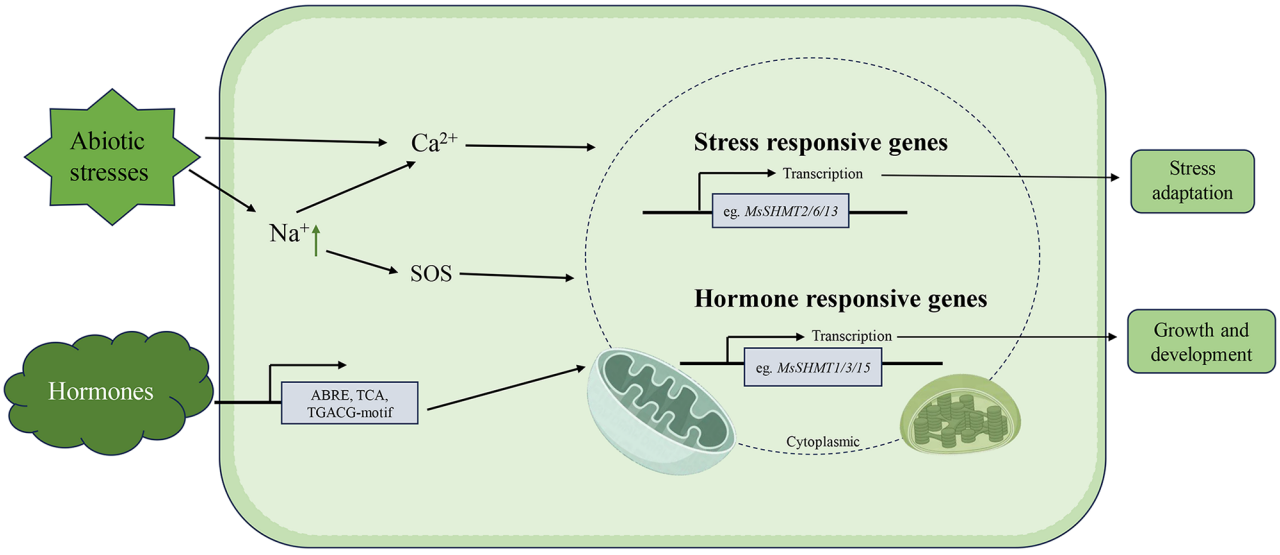


**Fig. 8** A working model of *MsSHMTs* response to hormones and abiotic stresses. Under abiotic stress, salt stress leads to a sudden increase in intracellular $Na^+$ content, and intracellular calcium signaling as well as SOS signaling are activated to increase the expression of genes such as *MsSHMT2/6/13* by binding to their promoters to mediate *M. sativa* response to abiotic stress. And hormone-responsive genes such as *MsSHMT1/3/15* may act in the regulation of *M. sativa* growth and development through transcription factors that bind to related *cis*-acting elements in the promoter regions of the genes

instance, while MeJA response elements were found in all *MsSHMT* genes, most genes did not show significant induction under MeJA treatment (Fig. 6). This may be attributed to the fact that the regulation of gene expression is not solely reliant on a single factor but rather involves the collaborative action of multiple transcription factors. Moreover, the limited availability of tissue, growth stages, and treatments may influence the interpretation of their relationships. Therefore, further experiments are necessary to elucidate the relationship between hormone responses and *cis*-acting elements.

As vital regulators of plant growth and development, *SHMT* gene family have been reported to respond to adverse environment in numerous species [7, 10, 29]. In *A. thaliana*, *AtSHMT1* collaborates with UBP16 (ubiquitin-specific protease) to control plasma membrane $Na^+/H^+$ antiporter activity under salt stress, thereby reducing $Na^+$ accumulation and enhancing plant tolerance to salt stress [42]. Overexpression of *OsSHMT* promotes scavenging of excessive harmful $H_2O_2$ by interacting with APX, Hsp70, ATP-synα, ATP-synβ, and MSCP, thus enhancing cold tolerance in *O. sativa* [43]. Additionally, studies have found that plant *SHMT* mitigates damage caused by low temperatures and drought by maintaining redox homeostasis and regulating stomatal closure [6]. In our study, *MsSHMT* genes responded to various stress stimuli consisting with the findings in *S. lycopersicum SHMT* research [7]. Specifically, *MsSHMT1/2/3/5/11/12* were significantly induced by salt stress; *MsSHMT2/4/13/15* were markedly induced by alkaline stress; while the expression levels of *MsSHMT1/3/6/7/8/15* were significantly upregulated under drought stress. Moreover, *MsSHMT4* exhibited sensitivity to high and low temperatures (Fig. 7). This indicates functional redundancy of *MsSHMTs* in mediating *M. sativa* responses to abiotic stresses. Considering these diverse stress response patterns, we hypothesize that the functional differences among these genes may be associated with *cis*-acting elements in their promoter regions, such as TC-rich repeat sequences, drought response elements (MBS), and low-temperature response elements (LTR). The presence of these *cis*-acting elements is likely responsible for the differential expression patterns of various *MsSHMT*s under specific stress conditions, implying their importance in regulating *MsSHMT* gene responses to environmental stresses. The differences in functionality among gene family members may be attributed to adaptive evolution. The functions of *MsSHMT* genes need to be further investigated in depth, and Fig. 8 shows a potential regulatory model of *MsSHMTs*.

## Conclusion

In general, 15 *SHMT* genes were identified in the *M. sativa* genome in this study. Physicochemical properties, gene and protein structures, and evolutionary relationships revealed structural and functional similarities and differences in *M. sativa SHMTs*. Tissue-specific analyses indicated that *MsSHMT* members play key housekeeping functions by regulating cellular metabolism during plant growth and development. In addition, *M. sativa SHMTs* are involved in hormonal responses and alleviating various abiotic stresses, especially salt stress and drought stress. In summary, this study aims to provide support for

further studies on the involvement of the *MsSHMT* gene family in *M. sativa* growth regulation and stress response, and to provide a theoretical basis for further exploration of the functions of plant *SHMT* members.

**Abbreviations**

| | |
|---|---|
| SHMT | Serine hydroxymethyltransferase |
| GDC | Glycine Decarboxylase Complex |
| ROS | Reactive oxygen species |
| SCN | Soybean cyst nematode |
| ER | Endoplasmic reticulum |
| Hsp70 | Heat shock protein 70 |
| HMM | Hidden Markov Model |
| qRT-PCR | Quantitative reverse transcription polymerase chain reaction |
| Ka/Ks | Nonsynonymous substitution rate/synonymous substitution rate |
| FPKM | Fragments Per Kilobase of transcript per Million mapped reads |

## Supplementary Information

The online version contains supplementary material available at https://doi.org/10.1186/s12864-024-10637-z.

Supplementary Material 1

**Acknowledgements**
We are grateful to members of our laboratory for helpful criticism and advice.

**Author contributions**
HLM and RG conceived and designed the experiment. RG and FQC performed the experiments. RG and LJC analyzed all the data. RG wrote he manuscript. HLM revised the manuscript. All of the authors read and approved the final manuscript.

**Funding**
This research was supported by the alfalfa breeding project (2022ZD0401102).

**Data availability**
All data generated or analyzed in this study are included in this published article and its supplementary material. The draft genome data of autotetraploid cultivated ('Xinjiang Daye') alfalfa was obtained from the figshare projects (https://figshare.com/projects/whole_genome_sequencing_and_assembly_of_Medicago_sativa/66380). Genome-wide transcriptome data of different alfalfa tissues were acquired from the NCBI short read archive database as accession SRP055547.

## Declarations

**Ethics approval and consent to participate**
Not applicable.

**Consent for publication**
Not applicable.

**Competing interests**
The authors declare no competing interests.

Received: 24 February 2024 / Accepted: 19 July 2024
Published online: 12 August 2024

**References**

1. Sa DW, Lu Q, Wang Z, Ge G, Sun L, Jia Y. The potential and effects of saline-alkali alfalfa microbiota under salt stress on the fermentation quality and microbial. BMC Microbiol. 2021;21(1):149.
2. Liu J, Tang L, Gao H, Zhang M, Guo C. Enhancement of alfalfa yield and quality by plant growth-promoting rhizobacteria under saline-alkali conditions. J Sci Food Agric. 2019;99(1):281–9.
3. Kaiwen G, Zisong X, Yuze H, Qi S, Yue W, Yanhui C, Jiechen W, Wei L, Huihui Z. Effects of salt concentration, pH, and their interaction on plant growth, nutrient uptake, and photochemistry of alfalfa (*Medicago sativa*) leaves. Plant Signal Behav. 2020;15(12):1832373.
4. Wang Y, Wang J, Guo D, Zhang H, Che Y, Li Y, Tian B, Wang Z, Sun G, Zhang H. Physiological and comparative transcriptome analysis of leaf response and physiological adaption to saline alkali stress across pH values in alfalfa (Medicago sativa). Plant Physiol Biochem. 2021;167:140–52.
5. Guiza M, Benabdelrahim MA, Brini F, Haddad M, Saibi W. Assessment of Alfalfa (*Medicago sativa* L.) cultivars for Salt Tolerance based on yield, growth, physiological, and biochemical traits. J Plant Growth Regul. 2022;41(8):3117–26.
6. Liu Y, Mauve C, Lamothe-Sibold M, Guerard F, Glab N, Hodges M, Jossier M. Photorespiratory serine hydroxymethyltransferase 1 activity impacts abiotic stress tolerance and stomatal closure. Plant Cell Environ. 2019;42(9):2567–83.
7. Liu Z, Pan X, Wang C, Yun F, Huang D, Yao Y, Gao R, Ye F, Liu X, Liao W. Genome-wide identification and expression analysis of serine hydroxymethyltransferase (*SHMT*) gene family in tomato (*Solanum lycopersicum*). PeerJ. 2022;10:e12943.
8. Lakhssassi N, Knizia D, El Baze A, Lakhssassi A, Meksem J, Meksem K, Proteomic. Transcriptomic, Mutational, and Functional Assays Reveal the Involvement of Both THF and PLP Sites at the *GmSHMT08* in Resistance to Soybean Cyst Nematode. Int J Mol Sci. 2022; 23(19).
9. Matsusaka H, Fukuda M, Elakhdar A, Kumamaru T. Serine hydroxymethyltransferase participates in the synthesis of cysteine-rich storage proteins in rice seed. Plant Sci. 2021;312:111049.
10. Hu P, Song P, Xu J, Wei Q, Tao Y, Ren Y, Yu Y, Li D, Hu H, Li C. Genome-wide analysis of serine hydroxymethyltransferase genes in Triticeae species reveals that *TaSHMT3A-1* regulates fusarium head blight resistance in wheat. Front Plant Sci. 2022; 13.
11. Ruszkowski M, Sekula B, Ruszkowska A, Dauter Z. Chloroplastic serine sydroxymethyltransferase from *Medicago truncatula*: a structural characterization. Front Plant Sci 2018; 9.
12. Gao R, Luo Y, Pan X, Wang C, Liao W. Genome-wide identification of SHMT family genes in cucumber (*Cucumis sativus* L.) and functional analyses of *CsSHMTs* in response to hormones and abiotic stresses. 3 Biotech. 2022;12(11):305.
13. Zhang J, Li M, Bryan AC, Yoo CG, Rottmann W, Winkeler KA, Collins Cassandra M, Singan V, Lindquist EA, Jawdy SS, et al. Overexpression of a serine hydroxymethyltransferase increases biomass production and reduces recalcitrance in the bioenergy crop Populus. Sustain Energ Fuels. 2019;3(1):195–207.
14. Nogues I, Sekula B, Angelaccio S, Grzechowiak M, Tramonti A, Contestabile R, Ruszkowski M. *Arabidopsis thaliana* serine hydroxymethyltransferases: functions, structures, and perspectives. Plant Physiol Biochem. 2022;187:37–49.
15. Yuan Y, Xu D, Xiang D, Jiang L, Hu H. Serine hydroxymethyltransferase 1 is essential for primary-Root growth at low-sucrose conditions. Int J Mol Sci 2022; 23(9).
16. Zhao X, Zeng Z, Cao W, Khan D, Ikram M, Yang K, Chen L, Li K. Co-overexpression of *AtSHMT1* and *AtFDH* induces sugar synthesis and enhances the role of original pathways during formaldehyde metabolism in tobacco. Plant Sci. 2021;305:110829.
17. Ye J, Chen W, Feng L, Liu G, Wang Y, Li H, Ye Z, Zhang Y. The chaperonin 60 protein SlCpn60α1 modulates photosynthesis and photorespiration in tomato. J Exp Bot. 2020;71(22):7224–40.
18. Wu XY, Zhou GC, Chen YX, Wu P, Liu LW, Ma FF, Wu M, Liu CC, Zeng YJ, Chu AE, et al. Soybean Cyst Nematode Resistance emerged via Artificial Selection of duplicated serine hydroxymethyltransferase genes. Front Plant Sci. 2016;7:998.
19. Wang AJ, Shu XY, Jing X, Jiao CZ, Chen L, Zhang JF, Ma L, Jiang YQ, Yamamoto N, Li SC, et al. Identification of rice (*Oryza sativa* L.) genes involved in sheath blight resistance via a genome-wide association study. Plant Biotechnol J. 2021;19(8):1553–66.
20. Fang C, Zhang P, Li L, Yang L, Mu D, Yan X, Li Z, Lin W. Serine hydroxymethyltransferase localised in the endoplasmic reticulum plays a role in scavenging $H_2O_2$ to enhance rice chilling tolerance. Bmc Plant Biol. 2020;20(1):236.
21. Chen H, Zeng Y, Yang Y, Huang L, Tang B, Zhang H, Hao F, Liu W, Li Y, Liu Y, et al. Allele-aware chromosome-level genome assembly and efficient transgene-free genome editing for the autotetraploid cultivated alfalfa. Nat Commun. 2020;11(1):2494.
22. Fu L, Niu B, Zhu Z, Wu S, Li W. CD-HIT: accelerated for clustering the next-generation sequencing data. Bioinformatics. 2012;28(23):3150–2.
23. Gasteiger E, Hoogland C, Gattiker A, Duvaud Se, Wilkins MR, Appel RD, Bairoch A. Protein Identification and Analysis Tools on the ExPASy Server. In:

*The Proteomics Protocols Handbook* Edited by Walker JM. Totowa, NJ: Humana Press; 2005: 571–607.
24. Bailey TL, Williams N, Misleh C, Li WW. MEME: discovering and analyzing DNA and protein sequence motifs. Nucleic Acids Res. 2006; 34(Web Server issue):W369–373.
25. Chen C, Chen H, Zhang Y, Thomas HR, Frank MH, He Y, Xia R. TBtools: an integrative Toolkit developed for interactive analyses of big Biological Data. Mol Plant. 2020;13(8):1194–202.
26. O'Rourke JA, Fu F, Bucciarelli B, Yang SS, Samac DA, Lamb JF, Monteros MJ, Graham MA, Gronwald JW, Krom N, et al. The *Medicago sativa* gene index 1.2: a web-accessible gene expression atlas for investigating expression differences between Medicago sativa subspecies. BMC Genomics. 2015;16(1):502.
27. Shen C, Du H, Chen Z, Lu H, Zhu F, Chen H, Meng X, Liu Q, Liu P, Zheng L, et al. The chromosome-level genome sequence of the Autotetraploid Alfalfa and Resequencing of Core Germplasms provide genomic resources for Alfalfa Research. Mol Plant. 2020;13(9):1250–61.
28. Zhang Y, Sun K, Sandoval FJ, Santiago K, Roje S. One-carbon metabolism in plants: characterization of a plastid serine hydroxymethyltransferase. Biochem J. 2010;430(1):97–105.
29. Lakhssassi N, Patil G, Piya S, Zhou Z, Baharlouei A, Kassem MA, Lightfoot DA, Hewezi T, Barakat A, Nguyen HT, et al. Genome reorganization of the *GmSHMT* gene family in soybean showed a lack of functional redundancy in resistance to soybean cyst nematode. Sci Rep-Uk. 2019;9(1):1506.
30. Zeng L, Tu XL, Dai H, Han FM, Lu BS, Wang MS, Nanaei HA, Tajabadipour A, Mansouri M, Li XL, et al. Whole genomes and transcriptomes reveal adaptation and domestication of pistachio. Genome Biol. 2019;20(1):79.
31. Cheng F, Sun R, Hou X, Zheng H, Zhang F, Zhang Y, Liu B, Liang J, Zhuang M, Liu Y, et al. Subgenome parallel selection is associated with morphotype diversification and convergent crop domestication in Brassica rapa and Brassica oleracea. Nat Genet. 2016;48(10):1218–24.
32. Nogués I, Sekula B, Angelaccio S, Grzechowiak M, Tramonti A, Contestabile R, Ruszkowski M. *Arabidopsis thaliana* serine hydroxymethyltransferases: functions, structures, and perspectives. Plant Physiol Biochem. 2022;187:37–49.
33. Xu YC, Guo YL. Less is more, natural loss-of-function mutation is a strategy for adaptation. Plant Commun. 2020;1(6):100103.
34. Wei K, Chen H. Comparative functional genomics analysis of *bHLH* gene family in rice, maize and wheat. BMC Plant Biol. 2018;18(1):309.
35. Ding F, Cui P, Wang Z, Zhang S, Ali S, Xiong L. Genome-wide analysis of alternative splicing of pre-mRNA under salt stress in *Arabidopsis*. BMC Genomics. 2014;15(1):431.
36. Moreno JI, Martín R, Castresana C. *Arabidopsis SHMT1*, a serine hydroxymethyltransferase that functions in the photorespiratory pathway influences resistance to biotic and abiotic stress. Plant J. 2005;41(3):451–63.
37. Kito K, Tsutsumi K, Rai V, Theerawitaya C, Cha-um S, Yamada-Kato N, Sakakibara S, Tanaka Y, Takabe T. Isolation and functional characterization of 3-phosphoglycerate dehydrogenase involved in salt responses in sugar beet. Protoplasma. 2017;254(6):2305–13.
38. Krishnamurthy P, Pothiraj R, Suthanthiram B, Somasundaram SM, Subbaraya U. Phylogenomic classification and synteny network analyses deciphered the evolutionary landscape of aldo–keto reductase (*AKR*) gene superfamily in the plant kingdom. Gene. 2022;816:146169.
39. Lee T, Orvosova M, Batzenschlager M, Bueno Batista M, Bailey PC, Mohd-Radzman NA, Gurzadyan A, Stuer N, Mysore KS, Wen J et al. Light-sensitive short hypocotyl genes confer symbiotic nodule identity in the legume *Medicago truncatula*. Curr Biol. 2024.
40. Nian L, Zhang X, Yi X, Liu X, Ain Nu, Yang Y, Li X, Haider FU, Zhu X. Genome-wide identification of ABA receptor *PYL/RCAR* gene family and their response to cold stress in *Medicago sativa* L. Physiol Mol Biol Plants. 2021;27(9):1979–95.
41. Anderssen S, Naômé A, Jadot C, Brans A, Tocquin P, Rigali S. AURTHO: Autoregulation of transcription factors as facilitator of cis-acting element discovery. Biochim Biophys Acta Gene Regul Mech. 2022;1865(5):194847.
42. Zhou H, Zhao J, Yang Y, Chen C, Liu Y, Jin X, Chen L, Li X, Deng XW, Schumaker KS, et al. Ubiquitin-specific protease16 modulates salt tolerance in Arabidopsis by regulating na(+)/H(+) antiport activity and serine hydroxymethyltransferase stability. Plant Cell. 2012;24(12):5106–22.
43. Mishra P, Jain A, Takabe T, Tanaka Y, Negi M, Singh N, Jain N, Mishra V, Maniraj R, Krishnamurthy SL et al. Heterologous expression of serine Hydroxymethyltransferase-3 from Rice confers tolerance to salinity stress in E. Coli and *Arabidopsis*. Front Plant Sci. 2019; 10.

## Publisher's Note